Available online at www.sciencedirect.com
ScienceDirect
Journal of the European Ceramic Society 29 (2009) 1641–1645
www.elsevier.com/locate/jeurceramsoc

Effects of milling on co-precipitated 3Y-PSZ powders

Erika Furlani, Eleonora Aneggi, Stefano Maschio *

Università di Udine, Dipartimento di Scienze e Tecnologie Chimiche, Via del Cotonificio 108-33100, Udine, Italy

Received 23 July 2008; received in revised form 23 September 2008; accepted 1 October 2008
Available online 7 November 2008

Abstract

The present research compares properties and behaviour of co-precipitated 3Y-PSZ powders submitted, after co-precipitation, to different milling treatments. The characteristics of the different products were evaluated by measurement of particle size distribution, thermogravimetric analysis, X-ray diffraction, specific surface area and scanning electron microscopy analysis. It has been demonstrated that 1 h of attrition milling enables the production of powders containing soft agglomerates of nanometric particles: the dispersing liquid used on milling has little influence. Crystallisation into a cryptocrystalline structure of the amorphous powder is achieved after 1 h of high energetic milling, avoiding thermal treatments.

Keywords: ZrO_2; Powders-chemical preparation; Milling

1. Introduction

Partially stabilized zirconia (PSZ) materials, sintered at high relative density, have high strength and good toughness thanks to the transformation toughening mechanism associated to the zirconia polymorphism.[1]

The catalytic properties of PSZ powders are also important since it has been demonstrated that they can be used for red-ox reactions at moderate temperature[2] and consequently also in the production of ceramic fuel cells.[3,4]

Zirconia materials can also be used as electric, electronic, magnetic and nuclear materials due to their good performances in these fields.[5–8]

Due to such a wide range of applications, zirconia-based materials have received a great deal of attention by researchers and a large number of papers are available on the subject, many of which dealing with the synthesis of zirconia powders and the production of zirconia monoliths and their properties. In all cases the first step is the production of powders and the effects of the properties of the powders on the performance of the material when it is in use. For example, the quality of gaseous emissions from most of the combustion processes used for energy production is greatly influenced by surface area and the catalytic activity of the powders used as catalysts. On the other hand, the production of submicronic grain-sized monoliths is impossible if the particles of the starting powders are not submicronic as well; secondly, if structural tools are to be produced, powders must possess a good sintering behaviour in order to minimize an undesired residual porosity.[9–11]

Depending on the application, either good sinterability or a stable surface area after severe temperature treatments are strictly required. Such characteristics are conflicting since powders which are able to maintain a high surface area after severe thermal treatments must not sinter.

Another feature of powder production is chemical homogenization which could be better achieved by chemical processes than by solid state reactions. Chemical processes require the preparation of solutions of precursors to be then converted into other specific products. During these critical preparation steps a great number of parameters, i.e. type of precursor (organic–inorganic), aspect (powder–solution), concentration, processing temperature and many others, must be carefully controlled. Unexpected events also causing the worsening of the characteristics of the powders cannot be excluded. A procedure that enables the reduction of such a large number of parameters making the production of powders with constant properties easier, could be worthwhile.

During the present research powders of 3Y-PSZ were produced by co-precipitation of zirconyl chloride octahydrate and yttrium nitrate pentahydrate. Co-precipitated products were divided into different batches: one was directly crystallised

* Corresponding author.
E-mail addresses: erika.furlani@uniud.it (E. Furlani), eleonora.aneggi@uniud.it (E. Aneggi), Stef.maschio@uniud.it (S. Maschio).

0955-2219/$ – see front matter © 2008 Elsevier Ltd. All rights reserved.
doi:10.1016/j.jeurceramsoc.2008.10.001

thermally, and the others were submitted to different milling procedures in order to optimize powder properties and preparation procedure.[12–14] The characteristics of the different products were evaluated by measurement of particle size distribution (PSD), thermogravimetric analysis (TGA), X-ray diffraction (XRD), specific surface area (BET) and scanning electron microscopy (SEM).

2. Experimental procedure

Co-precipitation of 3Y-PSZ precursors was made using $ZrOCl_2 \cdot 8H_2O$ (99.0% Aldrich Chem.), and the required amount of $Y(NO_3)_3 \cdot 5H_2O$ (99.9% Aldrich Chem.) which were dissolved in distilled water to give a 0.5-mol.% solution. This was poured, while stirring, into concentrated ammonia (28 wt%) at room temperature. The product was divided into two batches which were then processed as follows:

One batch was washed three times with de-ionized water dried at 80 °C in an oven, crushed in an agate mortar and submitted to BET, PSD, TGA, XRD and SEM. This powder was used as a reference and called A.

The second batch was washed three times with de-ionized water, then acetone–toluene–acetone (ATA)[15] and dried at 80 °C in an oven. This second powder was called B.

After drying, powder A was attrition milled for 1 or 2 h using 2-butanol as a dispersing liquid. The two resulting powders were respectively called A1 and A2.

After drying, powder B was divided into several further batches which were attrition milled for 1 or 2 h using three different dispersing liquids, i.e. ethanol, isopropanol and 2-butanol. The resulting powders were called, respectively, B1, B12, B2, B22, B3 and B32. For clarity names and processing parameters of the various powders are reported, together with their specific surface area and crystal structure, in Table 1.

For each milling process a high-density nylon container, zirconia/yttria (3 mol.%) spheres (sphere's diameter = 5 mm), 300 rpm were used and the following parameters were set: jar volume = 311 cm^3, amount of alcohol = 70 cm^3, amounts of balls = 480 g and amount of powder = 30 g. After milling, powders were dried in the oven at 80 °C and then tested by BET, PSD, XRD, SEM and, at the end, TGA.

As a further experiment, the dried B3 powder was milled with a high-energy spex mill for 1, 2, 4 and 8 h. The resulting powders were called respectively B3S1, B3S2, B3S4 and B3S8 (see Table 1). For such experiments 3Y-TZP balls and jar were used and the following ratios were set: powder weight/balls weight = 1.22/17 and powder volume/jar volume = 0.20/47.5.

PSD was determined by an Horiba LA950 laser scattering particle size distribution analyzer: analyses were made in water and, before their analysis, all powders were sonicated for 3 min. For clarity of comprehension all PSD curves are represented with logarithmic abscissa. XRD patterns were recorded on a Philips X'Pert diffractometer setting the operation conditions at 40 kV and 40 mA using nickel-filtered Cu Kα1 radiation. Spectra were collected using a step size of 0.02° and a counting time of 40 s/angular abscissa in the range 20°–80°; BET was determined by a Sorptomatic Carlo Erba BET instrument using nitrogen as a percolating gas; the powder particles morphology was examined by an Assing EVO40 scanning electron microscope (SEM) and, after these tests, thermogravimetric analyses (TGA) were performed on a TA Q500 at a heating rate of 10 °C/min up to a temperature of 700 °C.

3. Results and discussion

The reference powder (A) has a total weight loss of 45.44% during the TGA between room temperature and 700 °C; the X-ray diffraction analysis, before and after this thermal treatment, show that the powder, initially amorphous, crystallises into the tetragonal structure; Fig. 1 reports the PSD of powders A, A1 and A2. It is showed that powder A has a bimodal PSD with a first small peak at 14 μm and a second, greater, with a maximum at 95 μm. On the other hand, A1 and A2 have similar monomodal PSD: each one displays a single peak with maximum around 2 μm. The SEM image of powder A (Fig. 2a) confirms the presence of both small and large particles whereas its specific surface area (BET) was measured at 252 m^2/g. This very high BET value must be red with great caution because

Table 1
Symbolic names, corresponding schematic preparation procedure, specific surface area and X-ray results of the powders prepared in the present work.

Symbolic name	Schematic preparation procedure	Specific surface area ($m^2\ g^{-1}$)	X-ray results
A	Washed three times with H_2O	252	Amorphous
A1	As A and then attrition milled for 1 h with 2-butanol	133	Amorphous
A2	As A and then attrition milled for 2 h with 2-butanol	97	Amorphous
B	Washed three times with H_2O and then with ATA	42	Amorphous
B1	As B and then attrition milled for 1 h with ethanol	95	Amorphous
B12	As B and then attrition milled for 2 h with ethanol	88	Amorphous
B2	As B and then attrition milled for 1 h with isopropanol	103	Amorphous
B22	As B and then attrition milled for 2 h with isopropanol	92	Amorphous
B3	As B and then attrition milled for 1 h with 2-butanol	113	Amorphous
B32	As B and then attrition milled for 2 h with 2-butanol	94	Amorphous
B3S1	As B3 and then spex milled for 1 h	28	Tetragonal (cryptocrystalline)
B3S2	As B3 and then spex milled for 2 h	33	Tetragonal (cryptocrystalline)
B3S4	As B3 and then spex milled for 4 h	31	Tetragonal (cryptocrystalline)
B3S8	As B3 and then spex milled for 8 h	37	Tetragonal (cryptocrystalline)

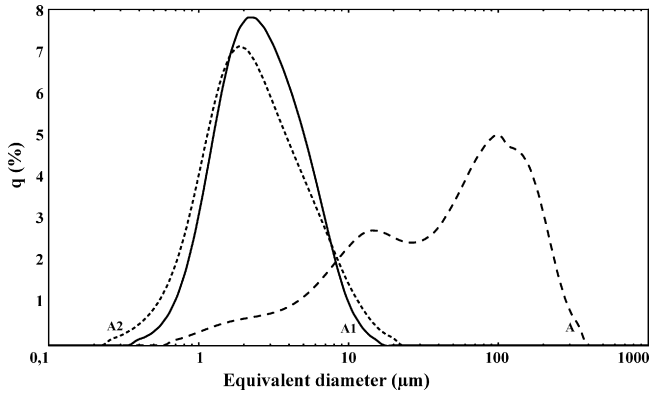

Fig. 1. Particles size distribution (PSD) curves of powders A, A1 and A2.

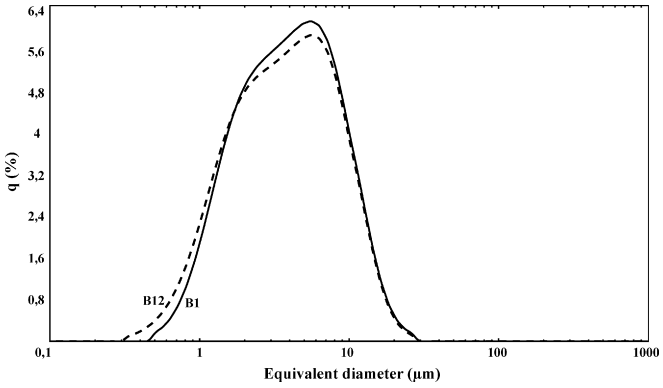

Fig. 3. Particles size distribution (PSD) curves of powders B1 and B12.

it is a reasonable consequence of the great amounts of volatile substances entrapped in the powder particles. In fact, before the BET test, powders must be degassed. Powder A has been degassed for a time twice longer than for all the other batches. Nevertheless it continues to release gases during the test. Consequently the resulting number is not too much reliable.

Table 1 also displays BET values and X-ray results of all the powders submitted to the corresponding preparation procedure. Comparing such values, thermal behaviour, PSD and SEM images of B1, B2 and B3 with those of B12, B22 and B32 it is possible to evaluate the influence of the liquid used for milling and then of milling time, on powder properties.

All the above powders are amorphous with surface areas of similar magnitude order. Fig. 3 shows the PSD curves of B1 and B12; it can be seen that they are close to one another (those of B2, B22, B3 and B33 show a trend not greatly different from that reported in Fig. 3). Fig. 4 shows the TGA curves of powders B1, B3 and B3S1. The one of B2 is practically overlapped to B1 and therefore, for clarity, not reported; it can be observed that the total weight loss of A (45.44%) is sensibly lowered after 1 h of milling (cfr B1-B3) (this result is already documented in an earlier paper),[16] independent of the alcohol used. Furthermore, the use of ethanol (powder B1) should be preferred since it is less dangerous than the two others against environment and human health. Changes, are very slight for a longer milling time, thus showing that milling process must be preferably stopped after 1 h because longer times only favour a partial re-agglomeration of particles and cause a reduction of BET values. The weight

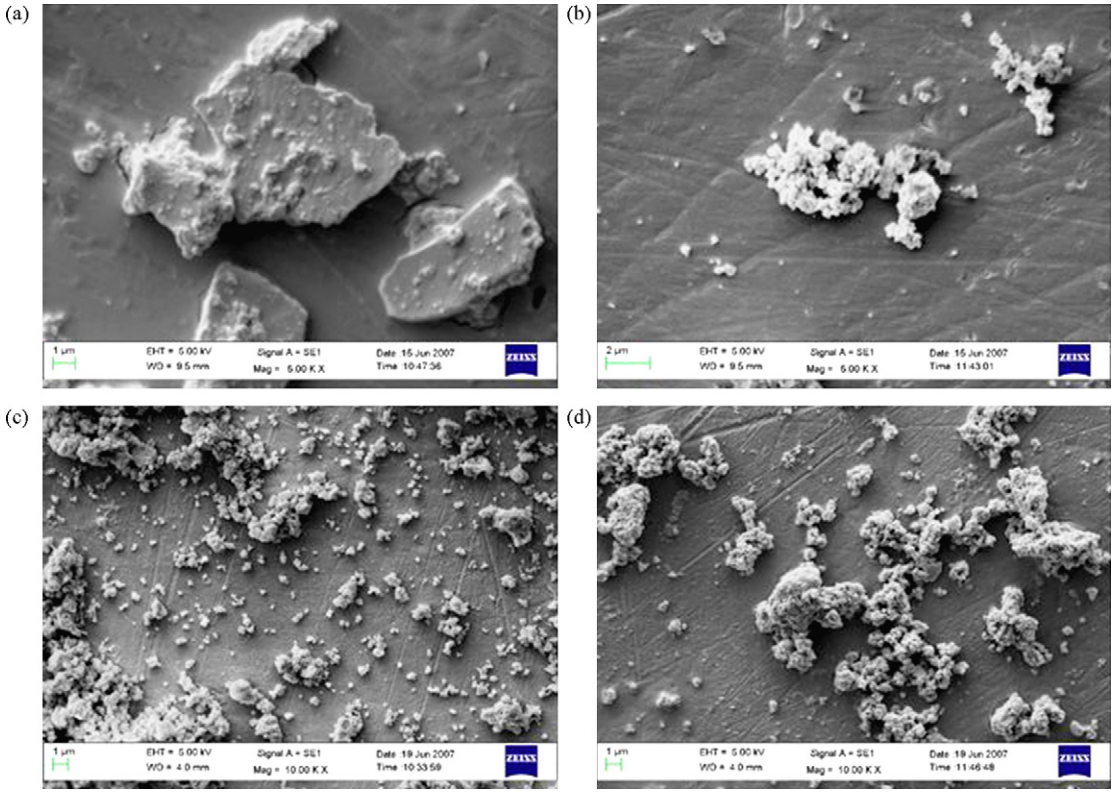

Fig. 2. SEM images of some of the powders prepared in the present study: (a) powder A (5000×); (b) powder B1 (5000×); (c) powder A1 (10,000×); (d) powder B3S1 (10,000×).

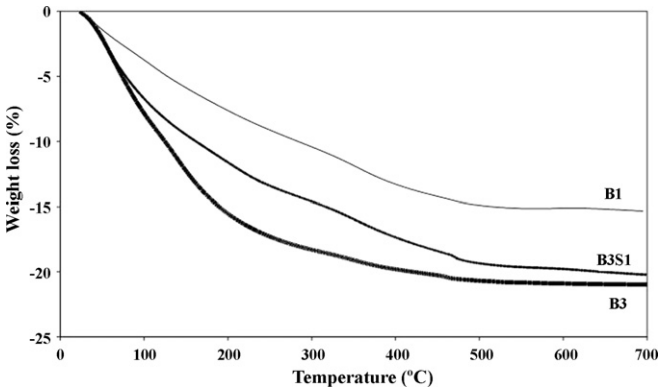

Fig. 4. TGA curves, between room temperature and 700 °C of powders B1, B3 and B3S1.

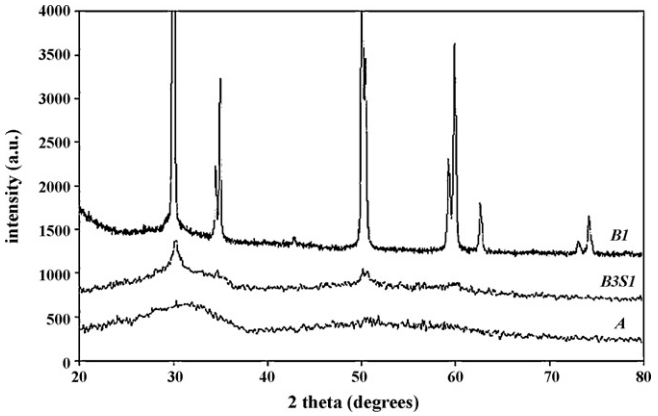

Fig. 5. X-ray diffraction patterns of powders A, B3S1 and B3 (after TGA), respectively.

loss reduction between A and milled products can be ascribed to the washing effect of the alcohol during milling: it facilitates the release of water entrapped in the precursors during the drying stage. More in particular, the specific behaviour of A is due to the presence of particles containing cavities filled with substances that decompose and evaporate; evaporation proceeds more slowly as the high partial pressure of the evolved gases in the cavities inhibit the complete decomposition of the entrapped material. Conversely, in the milled samples, most of the aggregates have been broken down; powder particles are in direct contact with the surrounding atmosphere so that water or other compounds can evaporate easily.

Fig. 2b is a SEM image of the powder B1 and shows agglomerates of nanometric particles. On the other hand, the PSD curve of the same powder displays the presence of micrometric particles. This apparent conflict could be explained taking into account the sonication time which is applied to the powders before the PSD measurements: the longer the time, the better the particle dispersion is. After a 3-min sonication time, agglomerates are only partially broken up into single particles, whereas part of them (the strongest) remains intact and is measured by the granulometer as a single particle.

Comparing properties and thermal behaviour of powders A, A1, A2 with those of powders B, B3 and B32, it is possible to evaluate the influence of the ATA process when powders are further attrition milled before their thermal crystallisation. Nevertheless, after the above discussion, the presence of A2 and B32, for such evaluation, results redundant since after 1 h of attrition milling, powders do not greatly change their properties. Table 1 shows that all the above powders are amorphous, being their specific surface area influenced by the ATA washing. In fact, it can be pointed out that the BET of A is 252 m^2/g whereas the one of B is 42 m^2/g and greatly changes from A to A1 and from B to B3, but A1 and B3 have values of same magnitude order. Similar trend was observed in the corresponding PSD curves which were narrowed after 1 h of milling, but longer milling time does not greatly improve the number of small particles. It is interesting to observe that 1 h of attrition milling transforms powders submitted to the ATA procedure into powders with similar properties to those similarly milled, but not submitted to the ATA washing. The thermogravimetric analysis did not show substantial differences between the thermal behaviour of A1 and that of B3. The SEM image of A1 (Fig. 2c) shows agglomerates of nanometric particles having different sizes.

Comparing properties and thermal behaviour of B3, with those of B3S1, B3S2, B3S4 and B3S8 it is possible to evaluate the influence of the time when powders B3 are milled with a Spex highly energetic mill. It is known that this type of mill is often used to induce mechanical alloying among several typologies of components.

In the present work the effect can be observed in Table 1 where it is shown that B3 is amorphous, whereas B3S1, B3S2, B3S4 and B3S8 show a cryptocrystalline tetragonal structure. As an example, Fig. 5 shows the X-ray diffraction patterns of powders A (amorphous), B3S1 (cryptocrystalline) and that of B3 (after the TGA test). The patterns of B3S2, B3S4 and B3S8 evidence the same structure as B3S1. Fig. 4 shows that the weight loss of B3 is greater than that of B3S1; the TGA curves acquired from B3S2, B3S4 and B3S8 are close to the one reported in the figure. The specific surface area, high in B3, drops dramatically after 1 h of milling and then it does not sensibly change. B3 has a narrow PSD curve with particles of size smaller than 20 μm whereas B3S1, B3S2, B3S4 and B3S8 have a large bimodal PSD with particles that can reach a size of 500 μm. In order to support the above statement, the PSD curve of B3S1 is reported in Fig. 6, those of B3S2, B3S4 and B3S8 do not greatly differ from that. The SEM image of B3S1 is shown in Fig. 2d: small as well as

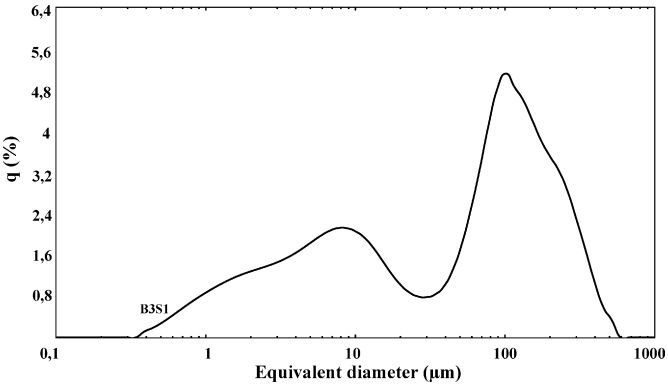

Fig. 6. Particles size distribution (PSD) curve of powder B3S1.

large hard agglomerates of nanometric particles are visible. The sonication time before the PSD measurements is not sufficiently long to destroy most of the agglomerates that are present in the powders which build up during the milling process. It may be concluded that highly energetic milling enable the production of cryptocrystalline powders just after 1 h of milling, but the high specific surface area of the starting products is reduced as well as is probably reduced its ability to sinter[17,18] due to the formation of large, strong agglomerates of particles.

4. Conclusions

An 1 h of attrition milling before calcination of co-precipitated 3Y-PSZ powders enables the production of powders with agglomerated nanometric particles. Ethanol, isopropanol or 2-butanol can be used as milling liquid, the choice made on the grounds of considerations regarding the environmental impact since powder properties are not greatly influenced by the type of liquid used during the milling stage. If powders are attrition milled after co-precipitation, also the ATA washing of the co-precipitated product could be avoided.

Attrition milled powders crystallise into the tetragonal structures (cryptocrystalline), after a 1 h milling with a Spex mill without any thermal treatment, but such powders have large PSD spectra, low BET and contain large hard agglomerates.

References

1. Garvie, R. C., Hannink, R. H. and Pascoe, R. T., Ceramic steel. *Nature*, 1975, **258**, 703–704.
2. Arai, H. and Machida, M., Properties of Pd-supported catalysts for catalytic combustion. *Catal. Today*, 1996, **28**, 250–254.
3. Holtappels, P. and Bagger, C., Fabrication and performance of advanced multi-layer SOFC cathodes. *J. Eur. Ceram. Soc.*, 2002, **22**(1), 41–48.
4. Zhitomirsky, I. and Petric, A., Electrophoretic deposition of ceramic materials for fuel cell applications. *J. Eur. Ceram. Soc.*, 2000, **20**(12), 2055–2061.
5. Gibson, I. R., Dransfield, G. P. and Irvine, J. T. S., Influence of yttria concentration upon electrical properties and susceptibility to ageing of yttria-stabilised zirconias. *J. Eur. Ceram. Soc.*, 1998, **18**(6), 661–667.
6. Degueldre, C., Pouchon, M., Döbeli, M., Sickafus, K., Hojou, K., Ledergerber, G. and Abolhassani-Dadras, S., Behaviour of implanted xenon in yttria-stabilised zirconia as inert matrix of a nuclear fuel. *J. Nucl. Mater.*, 2001, **289**(1/2), 115–121.
7. Grynszpan, R. I., Saudé, S., Anwand, W. and Brauer, G., Positron annihilation investigation and nuclear reaction analysis of helium and oxygen-implanted zirconia. *Nucl. Inst. Meth. Phys. Res. B*, 2005, **241**(1–4), 526–530.
8. Xu, S. Y., Huang, X. J., Ong, C. K., Lim, S. L., Chang, Y. L., Yang, Z., Li, Z. W. and Nie, H. B., Yttria-stabilized zirconia: a suitable substrate for c-axis preferred Nd–Fe–B thin films fabricated by pulsed-laser deposition. *J. Magn. Magn. Mater.*, 2000, **222**(1/2), 182–188.
9. Taha, M., Paletto, J., Jorand, Y., Fantozzi, G., Samdi, A., Jebrouni, M. and Durand, B., Compaction and sintering behaviour of zirconia powders. *J. Eur. Ceram. Soc.*, 1995, **15**, 759–768.
10. Chiou, Y. H. and Lin, S. T., Influences of powder preparation routes on the sintering behaviour of doped ZrO_2–3 mol.%Y_2O_3. *Ceram. Int.*, 1997, **23**, 171–177.
11. Dodd, A. C. and McCormick, P. G., Solid-state chemical synthesis of nanoparticulate zirconia. *Acta Mater.*, 2001, **49**, 4215–4220.
12. Farnè, G., Genel Ricciardiello, F., Kucich Podda, L. and Minichelli, D., Innovative milling of ceramic powders: influence on sintering zirconia alloys. *J. Eur. Ceram. Soc.*, 1999, **19**, 347–353.
13. Dodd, A. C., Tsuzuki, T. and McCormick, P. G., Nanocrystalline zirconia powders synthesised by mechanochemical processing. *Mater. Sci. Eng.*, 2001, **A301**, 54–58.
14. Yuan, Y., Wang, X. and Xiao, P., Attrition milling of metallic-ceramic particles in acetyl-acetone. *J. Eur. Ceram. Soc.*, 2004, **24**, 2233–2240.
15. Bi-Shiu, C., Hsu, W. Y. and Duh, J. G., Dehydration of synthesized calcia-stabilized zirconia from a coprecipitation process. *J. Mater. Sci. Lett.*, 1986, **5**, 931–934.
16. Maschio, S., Piras, A., Schmid, C. and Lucchini, E., Effects of attrition milling on precursors of Al_2O_3 and 12Ce-TZP powders. *J. Eur. Ceram. Soc.*, 2001, **21**(5), 589–594.
17. Maschio, S. and Trovarelli, A., Powders preparation and sintering behaviour of ZrO_2–Ce (20%mol) TZP solid solutions prepared by various methods. *Trans. Br. Ceram. Soc.*, 1995, **94**(5), 191–195.
18. Maschio, S., Lucchini, E. and Bachiorrini, A., Sintering behaviour of mechanically alloyed and coprecipitated 12Ce-PSZ powders. *J. Mater. Sci.*, 1998, **33**, 3437–3441.